GEOPHYSICS, VOL. 60, NO. 1 (JANUARY-FEBRUARY 1995); P. 268–284, 17 FIGS.

Normal moveout from dipping reflectors in anisotropic media

Ilya Tsvankin*

ABSTRACT

Description of reflection moveout from dipping interfaces is important in developing seismic processing methods for anisotropic media, as well as in the inversion of reflection data. Here, I present a concise analytic expression for normal-moveout (NMO) velocities valid for a wide range of homogeneous anisotropic models including transverse isotropy with a tilted in-plane symmetry axis and symmetry planes in orthorhombic media.

In transversely isotropic media, NMO velocity for quasi-*P*-waves may deviate substantially from the isotropic cosine-of-dip dependence used in conventional constant-velocity dip-moveout (DMO) algorithms. However, numerical studies of NMO velocities have revealed no apparent correlation between the conventional measures of anisotropy and errors in the cosine-of-dip DMO correction ("DMO errors"). The analytic treatment developed here shows that for transverse isotropy with a vertical symmetry axis, the magnitude of DMO errors is dependent primarily on the difference between Thomsen parameters ε and δ. For the most common case, $\varepsilon - \delta > 0$, the cosine-of-dip–corrected moveout velocity remains significantly larger than the moveout velocity for a horizontal reflector. DMO errors at a dip of 45 degrees may exceed 20–25 percent, even for weak anisotropy. By comparing analytically derived NMO velocities with moveout velocities calculated on finite spreads, I analyze anisotropy-induced deviations from hyperbolic moveout for dipping reflectors.

For transversely isotropic media with a vertical velocity gradient and typical (positive) values of the difference $\varepsilon - \delta$, inhomogeneity tends to reduce (sometimes significantly) the influence of anisotropy on the dip dependence of moveout velocity.

INTRODUCTION

Conventional methods of seismic processing and interpretation are designed for isotropic velocity fields and, therefore, are subject to error in anisotropic media. It has been shown that elastic anisotropy may seriously distort the results of velocity analysis, normal-moveout (NMO) correction and stacking, migration, etc. (Banik, 1984; Thomsen, 1986; Tsvankin and Thomsen, 1994; Sams et al., 1993; Larner and Cohen, 1993; among others). Clearly, dip-moveout processing cannot be an exception because most existing algorithms rely on the behavior of moveout velocity with reflector dip established for isotropic models (Levin, 1971):

$$V_{\text{nmo}}(\phi) = V_{\text{nmo}}(0)/\cos\phi, \tag{1}$$

where ϕ is the dip angle. For homogeneous isotropic media, reflection moveout is purely hyperbolic, and equation (1) is exact for any spread length.

It is well known that anisotropy may distort the normal (short-spread) moveout velocity for horizontal reflectors as well as enhance deviations from hyperbolic moveout (Banik, 1984; Thomsen, 1986; Tsvankin and Thomsen, 1994). Therefore, it is natural to expect formula (1) to become inaccurate in the presence of anisotropy.

Levin (1990) modeled *P*-wave reflection moveout for dipping reflectors beneath homogeneous transversely isotropic media with two different orientations of the axis of symmetry (for brevity, I will omit the qualifiers in "quasi-*P*-wave" and "quasi-*SV*-wave"). He showed that if the axis is perpendicular to the reflector, isotropic dip-moveout (DMO) formula (1) holds with good accuracy. However, if the symmetry axis is kept vertical, the error of equation (1) for one of the models in Levin's study (the shale-limestone) reaches almost 40 percent at 60-degree dip. For the other three media used by Levin, the errors were relatively small,

Manuscript received by the Editor August 13, 1993; revised manuscript received June 10, 1994.
*Center for Wave Phenomena, Colorado School of Mines, Golden, CO 80401.

although one of the models (Cotton Valley shale) may be considered even more "anisotropic" with respect to P-waves than the shale-limestone. Indeed, anisotropic parameters ε and δ (Thomsen, 1986) for the shale-limestone are $\varepsilon = 0.134$, $\delta = 0$, while for Cotton Valley shale $\varepsilon = 0.135$, $\delta = 0.205$. Small errors for the other two models (Pierre Shale and Berea sandstone) are not surprising since both are characterized by very weak P-wave anisotropy. It is also important to mention that Levin has not found noticeable nonhyperbolic moveout on common-midpoint (CMP) gathers with a spread length equal to the distance from the CMP to the reflector.

Recently, it has been recognized that depth-variable velocity may have a significant impact on dip-moveout processing. However, existing DMO algorithms built for depth-variable velocity fields still ignore anisotropy (e.g., Hale and Artley, 1993). The combined influence of anisotropy and inhomogeneity on DMO has been studied by Larner (1993), who has performed calculations similar to those of Levin (1990) but for "factorized" transversely isotropic models with a vertical velocity gradient ("factorized" means that the ratios of the elastic constants are independent of spatial position). The main conclusion of that work is that the DMO errors remain close to those found by Levin, provided isotropic DMO correction takes the velocity gradient into account.

Thus, the existing numerical results show no simple correlation between DMO errors and the "degree of anisotropy." Evidently, further insight into the character of DMO performance requires analytic description of reflection moveout from dipping planes in anisotropic media.

Another important aspect of this problem is the possibility of using the dip-dependence of normal-moveout (NMO) velocity in the inversion for the anisotropic parameters. Tsvankin and Thomsen (1995) showed that for transversely isotropic media, P-wave reflection moveout from horizontal interfaces is not sufficient to resolve the vertical velocity and anisotropic coefficients, even if long spreads (twice as large as the reflector depth) are used. Moveout from dipping reflectors makes it possible to extend the aperture of reflection data without recourse to large offsets (i.e., without using nonhyperbolic moveout).

Byun (1982) and Uren et al. (1990b) derived analytic expressions for normal-moveout velocity from dipping reflectors in elliptically anisotropic models. Uren et al. (1990b) also showed that, for elliptical anisotropy, reflection moveout remains hyperbolic irrespective of the orientation of the elliptical axes. However, elliptical anisotropy is no more than a special case of transverse isotropy, hardly typical for real rocks (Thomsen, 1986). Byun (1984) obtained an analytic expression for normal-moveout velocity in general transversely isotropic media by applying a local elliptical fit to the wavefront. The results discussed below show that Byun's formula deviates from the exact NMO velocity for nonelliptical models.

Here, I derive a formula for normal-moveout velocity valid for many anisotropic models of practical importance. For weak transverse isotropy with a vertical symmetry axis, this exact expression for NMO velocity is transformed into a simple function of the anisotropies ε and δ. I then compare the exact and weak-anisotropy expressions for NMO velocity with the moveout velocity calculated from $t^2 - x^2$ curves on conventional short spreads to verify analytic solutions and to estimate the influence of nonhyperbolic moveout. For values of ε and δ believed to be typical for real rocks, the cosine-of-dip-corrected moveout velocity remains significantly higher than the NMO velocity for a horizontal reflector. Finally, I use Larner's (1993) ray-tracing algorithm to analyze the combined influence of transverse isotropy and vertical velocity gradient on P-wave NMO velocity from dipping reflectors.

NORMAL-MOVEOUT VELOCITY IN ANISOTROPIC MEDIA

Let us consider a CMP gather over a homogeneous anisotropic medium; the CMP line is perpendicular to the strike of the reflector (Figure 1). The only assumption made about anisotropy at this stage is that the phase and group velocity vectors do not deviate from the sagittal (incidence) plane, i.e., the sagittal plane is a plane of symmetry. For instance, the present treatment is valid for any plane containing the symmetry axis in transversely isotropic media (plus the isotropy plane), as well as for symmetry planes in orthorhombic media.

Out-of-plane phenomena cannot be neglected if the sagittal plane lies outside symmetry planes in azimuthally anisotropic media; still, the formula derived below remains a good approximation if azimuthal anisotropy is weak. Azimuthally anisotropic models with orthorhombic symmetry caused by a combination of thin horizontal layering and vertical fracture systems with a low fracture density seem to be typical for sedimentary basins (Leary et al., 1990). Such media are characterized by relatively weak azimuthal anisotropy and more pronounced velocity variations in vertical planes. It is likely that for models of this type, the normal-moveout equation discussed here would be acceptable even outside symmetry planes.

Our goal is to find an analytic expression for the normal-moveout velocity in the CMP geometry (Figure 1):

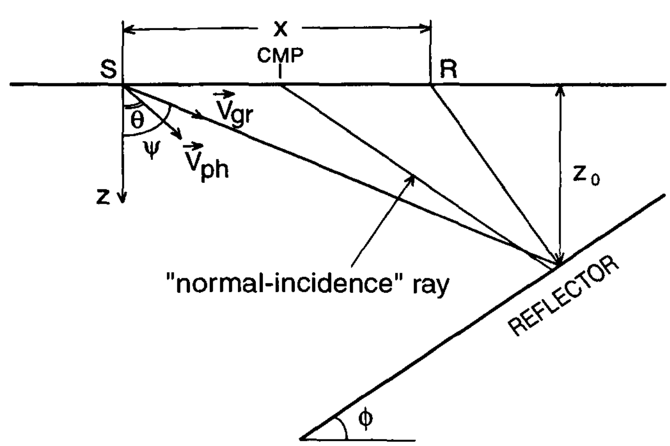

FIG. 1. Common-midpoint gather over a homogeneous anisotropic medium. $\mathbf{V}_{gr}$ and $\mathbf{V}_{ph}$ are the group and phase velocity vectors, respectively. For brevity, henceforth in the text $\mathbf{V}_{ph}$ is referred to just as $\mathbf{V}$. Note that the zero-offset ("normal-incidence") ray is not necessarily perpendicular to the reflector.

$$V^2_{nmo}(\phi) = \lim_{x \to 0} \frac{d(x^2)}{d(t^2)}. \quad (2)$$

For models with a horizontally homogeneous overburden, the ray parameter does not change between the reflector and the surface. In this case, it is convenient to represent the NMO velocity in the following way (Hale et al., 1992; Larner, 1993),

$$V^2_{nmo}(\phi) = \frac{2}{t_0} \lim_{h \to 0} \frac{dh}{dp}, \quad (3)$$

where $|h| = x/2$ is half the source-receiver offset ($h > 0$ in the down-dip direction), t_0 is the two-way traveltime along the zero-offset ("normal-incidence") ray, and p is the ray parameter. Note that the zero-offset ray ($h = 0$) is not necessarily perpendicular to the reflector in the presence of anisotropy; it is the phase-velocity vector associated with the zero-offset ray that is normal to the reflector.

Normal-moveout velocity (3) is derived under the assumption that the reflection point dispersal can be ignored (Hale et al., 1992). As shown in Hubral and Krey (1980, Appendix D), the difference between the true (specular) and zero-offset reflection points changes only the quartic and higher-order moveout terms and does not influence NMO velocity; their conclusion holds for anisotropic media as well. This implies that we can use z_0 (Figure 1) as the depth of the zero-offset reflection point. Then $h = z_0 (\tan \psi - \tan \psi_n)$, where ψ_n and ψ are the group-velocity (ray) angles for the zero-offset and nonzero-offset rays, respectively. Now equation (3) becomes

$$V^2_{nmo}(\phi) = \frac{2z_0}{t_0} \lim_{h \to 0} \frac{d \tan \psi}{dp}. \quad (4)$$

To evaluate equation (4), we use the general relation between group and phase velocities in anisotropic media (Berryman, 1979)

$$\mathbf{V}_{gr} = \frac{\partial(kV)}{\partial k_x}\mathbf{x} + \frac{\partial(kV)}{\partial k_y}\mathbf{y} + \frac{\partial(kV)}{\partial k_z}\mathbf{z},$$

where $\mathbf{k}$ is the wave vector with magnitude k, and V_{gr} and V are the group and phase velocities, respectively. If the incidence plane $[x, z]$ is both a plane of symmetry and the dip plane of the reflector, group- and phase-velocity vectors for CMP reflections remain in the vertical plane and depend only on the in-plane phase angle θ (we measure θ from the z-axis, see Figure 1). Therefore, group velocity may be represented as

$$\mathbf{V}_{gr} = \left(V \sin \theta + \frac{dV}{d\theta} \cos \theta\right)\mathbf{x} + \left(V \cos \theta - \frac{dV}{d\theta} \sin \theta\right)\mathbf{z}. \quad (5)$$

Note that the vertical axis is not necessarily an axis of symmetry. From equation (5), the group angle ψ is given by

$$\tan \psi = \frac{\tan \theta + \frac{1}{V}\frac{dV}{d\theta}}{1 - \frac{\tan \theta}{V}\frac{dV}{d\theta}}. \quad (6)$$

The derivative $d(\tan \psi)/dp$ in equation (4) may be written as

$$\frac{d \tan \psi}{dp} = \frac{d \tan \psi}{d\theta}\frac{d\theta}{dp}.$$

Using equation (6), we find

$$\frac{d \tan \psi}{d\theta} = \frac{1 + \frac{1}{V}\frac{d^2V}{d\theta^2}}{\cos^2 \theta \left(1 - \frac{\tan \theta}{V}\frac{dV}{d\theta}\right)^2}.$$

Since $p = \sin \theta / V$,

$$\frac{d\theta}{dp} = \frac{V}{\cos \theta \left(1 - \frac{\tan \theta}{V}\frac{dV}{d\theta}\right)},$$

then

$$\frac{d \tan \psi}{dp} = \frac{V\left(1 + \frac{1}{V}\frac{d^2V}{d\theta^2}\right)}{\left[\cos \theta \left(1 - \frac{\tan \theta}{V}\frac{dV}{d\theta}\right)\right]^3}. \quad (7)$$

The vertical distance from the zero-offset reflection point to the surface is given by

$$z_0 = \tfrac{1}{2} V_{gr}(\psi_n)\, t_0 \cos \psi_n.$$

Using expression (5) for group velocity yields

$$z_0 = \tfrac{1}{2} V t_0 \cos \theta \left(1 - \frac{\tan \theta}{V}\frac{dV}{d\theta}\right).$$

Since the phase angle θ for the zero-offset ray is equal to the dip angle ϕ, z_0 becomes

$$z_0 = \tfrac{1}{2} V(\phi)\, t_0 \cos \phi \left(1 - \frac{\tan \phi}{V(\phi)}\frac{dV}{d\theta}\right), \quad (8)$$

where the derivative $dV/d\theta$ should be calculated at the angle ϕ.

Substituting equations (7) and (8) into formula (4) for NMO velocity, we finally obtain

$$V_{nmo}(\phi) = \frac{V(\phi)}{\cos \phi} \frac{\sqrt{1 + \frac{1}{V(\phi)}\frac{d^2V}{d\theta^2}}}{1 - \frac{\tan \phi}{V(\phi)}\frac{dV}{d\theta}}, \quad (9)$$

where both derivatives of phase velocity should be evaluated at the dip angle ϕ.

Equation (9) is valid for NMO velocity of P- and S-waves in symmetry planes of arbitrary anisotropic media. Difficulties in application of formula (9) can be expected only in anomalous areas near shear-wave singularities and cusps, where the group-velocity function is multivalued. This expression is relatively simple to use because it does involve just the phase-velocity function, not the components of the group-velocity vector of the zero-offset ray (note that the angle between the zero offset ray and vertical is generally different from ϕ). For example, it can be used in symmetry planes of orthorhombic media just by substituting the appropriate phase velocity function and its derivatives.

From equation (9), the result of the conventional isotropic dip-moveout correction

$$V_{\text{corr}}(\phi) = V_{\text{nmo}}(\phi) \cos \phi \tag{10}$$

may be far different from the NMO velocity for a horizontal reflector $V_{\text{nmo}}(0)$, if anisotropy is present. Below, I examine the behavior of the normal-moveout velocity and performance of the isotropic DMO correction for transversely isotropic media.

TRANSVERSE ISOTROPY WITH A TILTED AXIS OF SYMMETRY

Levin (1990) showed numerically that the cosine-of-dip correction remains accurate in the case when the symmetry axis is perpendicular to the reflector. Equation (9) gives a clear analytic explanation for this result. If the reflector's normal coincides with the symmetry direction, then $dV/d\theta$ at the dip angle is zero, and formula (9) reduces to

$$V_{\text{nmo}}(\phi) = \frac{V(\phi)}{\cos \phi} \sqrt{1 + \frac{1}{V(\phi)} \frac{d^2V}{d\theta^2}}. \tag{11}$$

The values of $V(\phi)$ and $d^2V/d\theta^2$ at any dip correspond to the symmetry direction and, therefore, are independent of ϕ. Hence, equation (11) coincides with the isotropic equation (1)

$$V_{\text{nmo}}(\phi) = V_{\text{nmo}}(0)/\cos \phi.$$

This means that the isotropic DMO correction holds if the symmetry axis is perpendicular to the reflector. However, this result is derived for normal (zero-spread) moveout velocities rather than for moveout velocities measured on finite spreads. If the medium above the reflector is homogeneous and isotropic, reflection moveout on CMP gathers is purely hyperbolic, and equation (1) is exact irrespective of the maximum offset. In the presence of anisotropy, however, moveout is generally nonhyperbolic (Tsvankin and Thomsen, 1994), and equation (11) may become inaccurate with increasing spread length. Although the spreads used by Levin (1990) are not long (equal to the normal distance to the reflector), his results for the models with the symmetry axis perpendicular to the reflector show small errors in the cosine-of-dip relationship (1), indicative of the influence of nonhyperbolic moveout on the moveout velocity.

While dip dependence of the NMO velocity is not distorted by the anisotropy when the symmetry axis is perpendicular to the reflector, the value of $V_{\text{nmo}}(0)$ is not the same as the NMO velocity for isotropic media. The P-wave $V_{\text{nmo}}(0)$ depends on the anisotropic parameter δ, which is responsible for P-wave velocity near the symmetry axis (Thomsen, 1986); this will be discussed in more detail below.

Application of formula (9) remains straightforward in a more general case when the symmetry axis is tilted at an arbitrary angle. Phase velocity in transversely isotropic media is usually expressed through the angle between the phase-velocity vector and the symmetry axis. The formula for the P-wave phase velocity in standard notation (using the elastic coefficients c_{ij} and density ρ) can be found, for instance, in White (1983):

$$\begin{aligned} 2\rho V^2(\theta) = {} & (c_{11} + c_{44}) \sin^2 \theta + (c_{33} + c_{44}) \cos^2 \theta \\ & + \{[(c_{11} - c_{44}) \sin^2 \theta - (c_{33} - c_{44}) \cos^2 \theta]^2 \\ & + 4(c_{13} + c_{44})^2 \sin^2 \theta \cos^2 \theta\}^{1/2}. \end{aligned} \tag{12}$$

To get the SV-wave velocity, the plus sign in front of the radical should be replaced with a minus. Thomsen (1986) gives analogous formulas in his notation and transforms them into much simpler expressions for weakly anisotropic media. To use any of these velocity equations in the calculation of the NMO velocity (9), they should be evaluated at the angle between the symmetry axis and the reflector's normal.

TRANSVERSE ISOTROPY WITH A VERTICAL AXIS OF SYMMETRY

Levin (1990) points out that the orientations of the symmetry axis most likely to be encountered in practice are close to either the vertical or the normal to reflectors. In the previous section it was proved that in the latter case dip-dependence of normal-moveout velocity remains the same as in isotropic media. Therefore, although formula (9) allows for rather general anisotropy, in the following I concentrate on transversely isotropic media with a vertical symmetry axis, or vertical transverse isotropy (VTI).

I will characterize VTI by the vertical P- and S-wave velocities ($V_{P0} = \sqrt{c_{33}/\rho}$ and $V_{S0} = \sqrt{c_{44}/\rho}$), and the anisotropic parameters ε, δ, and γ, defined by Thomsen (1986):

$$\varepsilon \equiv \frac{c_{11} - c_{33}}{2c_{33}}, \tag{13}$$

$$\delta \equiv \frac{(c_{13} + c_{44})^2 - (c_{33} - c_{44})^2}{2c_{33}(c_{33} - c_{44})}, \tag{14}$$

$$\gamma \equiv \frac{c_{66} - c_{44}}{2c_{44}}. \tag{15}$$

P- and SV-wave propagation is described fully by four parameters: V_{P0}, V_{S0}, ε, and δ.

The SH-wave slowness surface and wavefront are elliptical with the phase velocity given (exactly) by

$$V_{SH}(\theta) = V_{S0}\sqrt{1 + 2\gamma \sin^2 \theta}. \tag{16}$$

Special cases: comparison with previous results

In this section, formula (9) is compared with analytic expressions for the normal-moveout velocity from a horizontal reflector beneath VTI media (Hake et al., 1984; Thomsen, 1986), and from dipping reflectors beneath elliptically anisotropic media (Byun, 1982; Uren et al., 1990b). Formula (9) and the P-wave moveout velocity computed from $t^2 - x^2$ curves are also compared with analytically based calculations for general transverse isotropy presented by Byun (1984).

In the case of a horizontal reflector ($\phi = 0$), equation (9) reduces to

$$V_{\mathrm{nmo}}(0) = V_0 \sqrt{1 + \frac{1}{V_0} \frac{d^2 V}{d\theta^2}}.$$

Using equation (12) to evaluate the second derivative of phase velocity and substituting expression (14) for δ, we find for the P-wave

$$V_{\mathrm{nmo}}(0)(P) = V_0 \sqrt{1 + 2\delta}, \tag{17}$$

which coincides with Thomsen's (1986) result. It should be emphasized that equation (17), along with the original equation (9), is valid for VTI media with an arbitrary degree of anisotropy, not just for weak transverse isotropy. When the symmetry axis is perpendicular to a dipping reflector, the P-wave NMO velocity is given just by equation (17) and the cosine-of-dip factor [equation (1)]. Similarly, we get Thomsen's expression for the zero-dip NMO velocity of the SV-wave.

For elliptical anisotropy,

$$V(\theta) = \sqrt{V_0^2 \cos^2\theta + V_{90}^2 \sin^2\theta},$$

where V_{90} is the horizontal velocity.

The NMO velocity (9) then becomes

$$V_{\mathrm{nmo}}(\phi) = \frac{V_{90}}{\cos\phi} \sqrt{\cos^2\phi + \frac{V_{90}^2}{V_0^2} \sin^2\phi}. \tag{18}$$

Equation (18) agrees with the normal-moveout formulas of Byun (1982) and Uren et al. (1990b). In elliptically anisotropic media, reflection moveout remains purely hyperbolic irrespective of reflector dip or the orientation of the elliptical axes (Uren et al., 1990b).

In general VTI media, equations for elliptical anisotropy are strictly valid only for the SH-wave. If the SH-wave phase velocity is parametrized by γ as in equation (16), formula (18) yields

$$V_{\mathrm{nmo}}(\phi)(SH) = \frac{V_{S0}\sqrt{1 + 2\gamma}}{\cos\phi} \sqrt{1 + 2\gamma \sin^2\phi}. \tag{19}$$

Since for the SH-wave $V_{\mathrm{nmo}}(0) = V_{S0}\sqrt{1 + 2\gamma}$, equation (19) may be represented as

$$V_{\mathrm{nmo}}(\phi)(SH) = \frac{V_{\mathrm{nmo}}(0)}{\cos\phi} \frac{V_{SH}(\phi)}{V_{S0}}, \tag{20}$$

$V_{SH}(\phi)$ is the SH-wave phase velocity at the dip angle. Therefore, for elliptical anisotropy the error of the cosine-of-dip–DMO correction is determined directly by phase velocity variations, i.e., the error is given just by the phase velocity at the dip angle divided by the vertical velocity.

I demonstrate below that the formula for elliptical anisotropy may lead to significant errors in the P-wave NMO velocity even for "almost" elliptically anisotropic models.

Byun (1984) generalized his elliptical normal-moveout formula for arbitrary transverse isotropy by applying a local elliptical fit to the wavefront. The resulting expression for the normal-moveout velocity involves the group velocity and group angle of the normal-incidence ray. The moveout velocity multiplied with the cosine of the angle ψ_n between the zero-offset ray and vertical ("emergence angle" in Byun's paper) Byun calls the "diffractor velocity." Figure 2 shows the P-wave moveout velocity for the limestone-sandstone model used in Byun's study with his normalization. The dotted curve is the analytic NMO velocity computed from formula (9); the solid curve is the moveout velocity recovered directly from traveltimes ($t^2 - x^2$ curves) calculated by a ray-tracing code over a spread of 1500 m. The distance from the CMP to the reflector in the traveltime calculations on this and all subsequent plots (except for Figure 16) is 3000 m [for a description of the algorithm used to calculate traveltimes, see Larner (1993)].

Figure 2 was designed to reproduce the result in Figure 6a of Byun's (1984) paper. However, with increasing dip the moveout velocities in Figure 2 become substantially higher than those computed by Byun; a similar discrepancy was found for the second model used in Byun's work. Since the analytic and numerical results in Figure 2 are close to each other (the small difference between the two curves will be explained below), it seems that Byun's formula deviates (at least for these two models) from the exact V_{nmo} for nonelliptical media.

We can only speculate about the reason for this inaccuracy. One of the assumptions made by Byun in his derivation is that V_{nmo} for VTI media can be found by fitting an ellipse

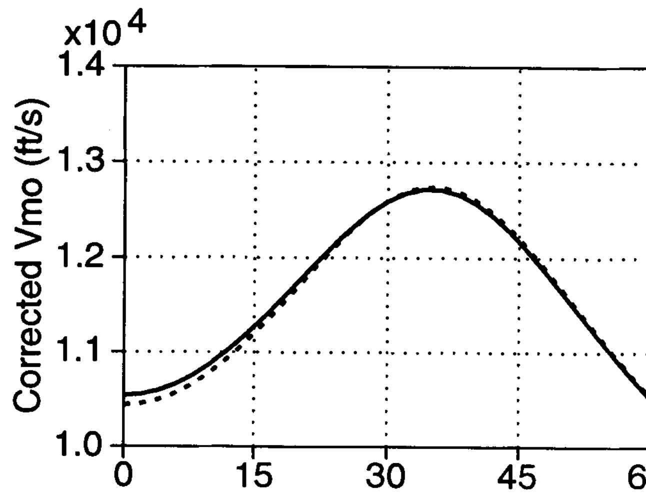

FIG. 2. P-wave moveout velocity calculated from formula (9) (dotted curve) and from traveltimes (solid curve) for the limestone-sandstone model from Byun (1984). Both curves are converted into the "diffractor velocities" as suggested by Byun. Model parameters are V_{P0} = 10 483 ft/s, V_{S0} = 5753 ft/s, $\varepsilon = 0.183$, $\delta = -0.004$.

with vertical and horizontal axes to the wavefront. It is possible that the correct moveout velocity at nonzero dips is given by a tilted fitted ellipse, even though the symmetry axis is vertical. However, this is no more than a tentative conclusion; the nature of the above discrepancy needs further investigation.

How many parameters determine the *P*-wave DMO signature?

This important question has to be answered before starting a systematic study of the behavior of NMO velocities in transversely isotropic media. In conventional notation, the *P*-wave phase velocity (12) is a function of four elastic coefficients: c_{11}, c_{33}, c_{13}, and c_{44}. This might lead one to believe that dip dependence of the *P*-wave V_{nmo} is also determined by four variables.

However, it is possible to cut down on the number of parameters by switching to Thomsen's (1986) notation. First, note that V_{P0} is just a scaling coefficient for the *P*-wave phase velocity, if V_{P0}/V_{S0}, ε, and δ are kept constant. Therefore, V_{P0} does not change the dependence of the *P*-wave normal-moveout velocity V_{nmo} on the dip angle ϕ. This conclusion is illustrated in Figure 3, which shows that the normalized *P*-wave NMO velocity $V_{nmo}(\phi)/V_{nmo}(0)$ (Figure 3b) is independent of the vertical velocity V_{P0}. The velocity in Figure 3 is the moveout velocity in equation (9) multiplied with cos ϕ, as it is conventionally done in the isotropic DMO correction.

Another parameter that can be eliminated from the *P*-wave dip-moveout problem is the shear-wave vertical velocity V_{S0} (or the ratio V_{P0}/V_{S0}). Although the *P*-wave phase velocity formally depends on four Thomsen parameters (V_{P0}, V_{S0}, ε, and δ), the contribution of V_{S0} is practically negligible.

Indeed, in the weak-anisotropy approximation, the *P*-wave phase velocity is a function just of V_{P0} and the anisotropic coefficients ε and δ (Thomsen, 1986). If anisotropy is not weak, Thomsen's velocity equation becomes inaccurate, but the *P*-wave phase velocity remains practically independent of V_{S0} (Tsvankin and Thomsen, 1994). Hence, even for a wide range of V_{S0}, the corresponding variations in the *P*-wave normal moveout are insignificant, as is supported by the result in Figure 4.

Thus, in VTI media the dip dependence of the *P*-wave NMO velocity is primarily a function of just two anisotropic coefficients ε and δ. More than that, in the next two sections I show that the angular behavior of the NMO velocity is mostly determined by a particular combination of these parameters; i.e., by the difference $\varepsilon - \delta$. If the symmetry axis is inclined, the NMO velocity is also dependent on the tilt angle.

Weak-anisotropy approximation for normal-moveout velocity

A convenient way to understand the influence of anisotropy on normal-moveout velocity is to use the weak-anisotropy approximation (WAA). Although WAA is no substitute for exact equations [such as formula (9)] in DMO correction, it can provide us with simple analytic relations elucidating

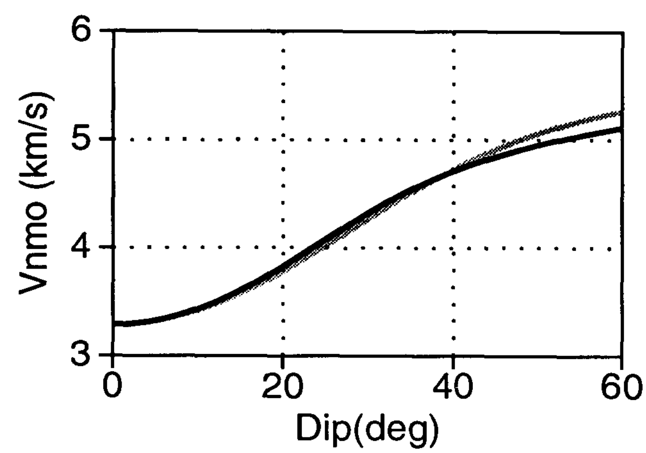

FIG. 4. Influence of V_{S0} on the cosine-of-dip-corrected *P*-wave normal-moveout velocity calculated from formula (9). The black curve corresponds to $V_{P0}/V_{S0} = 1.5$, the gray curve to $V_{P0}/V_{S0} = 2.5$. $V_{P0} = 3$ km/s, $\varepsilon = 0.3$, and $\delta = 0.1$ are the same for both curves.

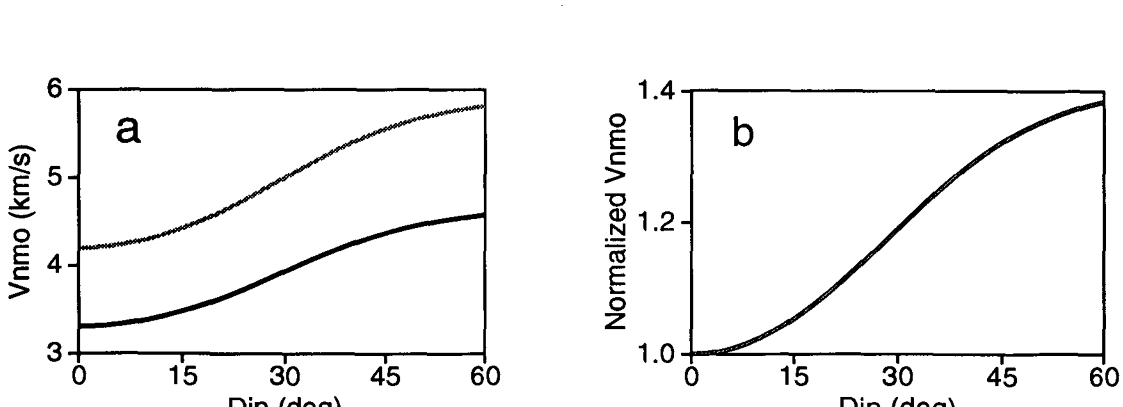

FIG. 3. Influence of V_{P0} on the cosine-of-dip-corrected *P*-wave normal-moveout velocity calculated from formula (9). The black curve corresponds to the shale-limestone model with $V_{P0} = 3.306$ km/s, $V_{S0} = 1.819$ km/s, $\varepsilon = 0.134$, $\delta = 0$. The gray curve is for the model with $V_{P0} = 4.200$ km/s, and the same V_{P0}/V_{S0}, ε, and δ. (a) NMO velocity without normalization; (b) NMO velocity normalized by the zero-dip value $V_{nmo}(0)$.

the dependence of the NMO velocity on the parameters ε and δ.

In the case of weak anisotropy ($\varepsilon \ll 1$, $\delta \ll 1$), phase velocities of P- and SV-waves can be significantly simplified by retaining only the terms linear in ε and δ. The P-wave phase velocity linearized in ε and δ is given by (Thomsen, 1986)

$$V_P(\theta) = V_{P0}(1 + \delta \sin^2 \theta \cos^2 \theta + \varepsilon \sin^4 \theta). \quad (21)$$

The derivatives of equation (21) needed in the expression for NMO velocity (9) are then

$$\frac{dV_P(\theta)}{d\theta} = V_{P0} \sin 2\theta (\delta \cos 2\theta + 2\varepsilon \sin^2 \theta),$$

$$\frac{dV_P^2(\theta)}{d\theta^2} = 2V_{P0} [\delta \cos 4\theta + 2\varepsilon \sin^2 \theta (1 + 2 \cos 2\theta)].$$

After substitution of the above weak-anisotropy equations into equation (9) and further linearization in ε and δ, we get

$$V_{\text{nmo}}(\phi) = \frac{V_P(\phi)}{\cos \phi} [1 + \delta + 2(\varepsilon - \delta) \sin^2 \phi (1 + 2 \cos^2 \phi)]. \quad (22)$$

$V_P(\phi)$ is the phase velocity given by equation (21). In the isotropic DMO correction, multiplication of $V_{\text{nmo}}(\phi)$ with $\cos \phi$ is supposed to convert the moveout velocity at dip ϕ into the moveout velocity for a horizontal reflector. Hence, the anisotropy-induced DMO error in the weak-anisotropy approximation is given by (again, only the terms linear in ε and δ are retained)

$$\frac{V_{\text{nmo}}(\phi) \cos \phi}{V_{\text{nmo}}(0)} = \frac{V_P(\phi)}{V_{P0}} \times [1 + 2(\varepsilon - \delta) \sin^2 \phi (1 + 2 \cos^2 \phi)]. \quad (23)$$

The structure of equation (23) suggests that the P-wave dip-moveout error in transversely isotropic media has two major components, which may be called the "elliptical error" and "nonelliptical error." Indeed, for elliptical anisotropy $\varepsilon = \delta$, and the error is determined just by angular variations in the P-wave phase velocity. This result has already been discussed in the previous section [equations (18) and (20)]. The second, nonelliptical component of the DMO error is the term containing the difference $\varepsilon - \delta$.

To compare the two components, I substitute the weak-anisotropy approximation for $V_P(\phi)$ in equation (21) into equation (23) and drop the terms quadratic in the anisotropies ε and δ. The dip-moveout error then becomes

$$\frac{V_{\text{nmo}}(\phi) \cos \phi}{V_{\text{nmo}}(0)} = 1 + \delta \sin^2 \phi + 3(\varepsilon - \delta) \sin^2 \phi (2 - \sin^2 \phi). \quad (24)$$

The nonelliptical error in the fully linearized expression (24) is represented by the last term. Analysis of the trigonometric coefficients in equation (24) shows that, unless $|\varepsilon - \delta| \ll |\delta|$, the nonelliptical term usually makes the most significant contribution to the total error. Thus, for typical values of the anisotropic coefficients, the difference $\varepsilon - \delta$ determines, to a large degree, the angular behavior of the P-wave NMO velocity. This conclusion is supported by exact numerical calculations in the next section.

Now we can explain the puzzling difference between the DMO signatures for the models of Cotton Valley shale and the shale-limestone (Levin, 1990; Larner, 1993). For Cotton Valley shale ($\varepsilon = 0.135$, $\delta = 0.205$), δ is positive, while $\varepsilon - \delta$ is small and negative. As a result, the two components of the DMO error in equations (23) and (24) almost cancel each other, and the accuracy of the isotropic DMO correction is quite satisfactory.

Figure 5 shows the comparison between the moveout velocity calculated directly from traveltimes ($t^2 - x^2$ curves) over a spread of 3000 m, the exact NMO velocity (9), and the weak-anisotropy normal-moveout approximation (22) for the model of Cotton Valley shale. All three curves display only small variations (~3–4 percent) in the corrected moveout velocity with angle, confirming the conclusion about the validity of the cosine-of-dip correction for this particular model. Though Cotton Valley shale has a large value of δ,

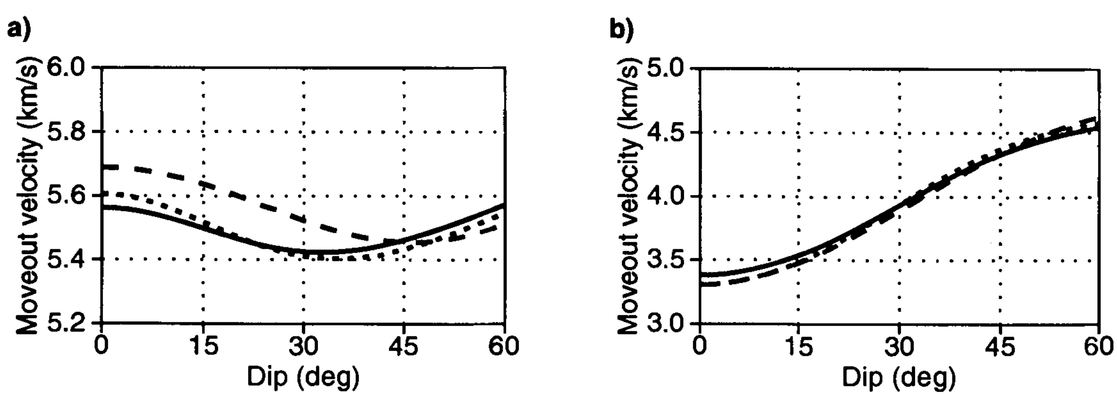

FIG. 5. Cosine-of-dip–corrected P-wave moveout velocity for (a) Cotton Valley shale and the (b) shale-limestone. The solid curve is the moveout velocity calculated from the traveltimes on a spread of 3000 m (the CMP-to-reflector distance is also 3000 m); the dotted curve is the exact NMO velocity computed from formula (9); the dashed curve is the weak-anisotropy approximation (22). Parameters of Cotton Valley Shale are V_{P0} = 4.721 km/s, V_{S0} = 2.890 km/s, ε = 0.135, δ = 0.205; for the shale-limestone, V_{P0} = 3.306 km/s, V_{S0} = 1.819 km/s, ε = 0.134, δ = 0.

the weak-anisotropy result is close to the exact NMO velocity (the difference is less than 2 percent).

For the shale-limestone ($\varepsilon = 0.134$, $\delta = 0$), a positive value of $\varepsilon - \delta$ leads to a pronounced increase in the cosine-of-dip corrected moveout velocity with dip angle. Note that the accuracy of the weak-anisotropy approximation for the shale-limestone is high. A systematic comparison between the weak-anisotropy approximation and the exact NMO velocity is presented in the next section.

Formula (9) can also be transformed into the weak-anisotropy approximation for the SV-wave normal-moveout velocity. Using the weak-anisotropy expression for the SV-wave phase velocity (Thomsen, 1986)

$$V_{SV}(\theta) = V_{S0}(1 + \sigma \sin^2 \theta \cos^2 \theta),$$

we obtain

$$V_{\text{nmo}}(\phi)(SV) = \frac{V_{SV}(\phi)}{\cos \phi} \times [1 + \sigma - 2\sigma \sin^2 \phi\, (1 + 2 \cos^2 \phi)], \quad (25)$$

where σ is the effective parameter introduced in Tsvankin and Thomsen (1994) to describe SV-wave propagation:

$$\sigma \equiv \left(\frac{V_{P0}}{V_{S0}}\right)^2 (\varepsilon - \delta).$$

Hence, the DMO signature for the SV-wave is mostly determined by just one anisotropic parameter–σ.

Equations (22) and (25) can be rewritten (not done here) for the more general case of transverse isotropy with a tilted axis of symmetry.

Dip-moveout signature for P-waves

Before doing a systematic analysis for vertical transverse isotropy, it is worthwhile to explain the small difference between the moveout velocity calculated directly from traveltimes ($t^2 - x^2$ curves), and NMO velocity from formula (9) in Figures 2 and 5. Since the moveout velocity was determined from a least-squares fit to $t^2 - x^2$ curves on a finite spread length, it could have been distorted by nonhyperbolic moveout, while the analytic NMO velocity describes purely hyperbolic moveout on very short spreads. To check out this possibility, Figure 5 is reproduced in Figure 6, but with the moveout velocity calculated on a much shorter spread (1000 m instead of 3000 m), reduced to just 1/3 of the distance from the CMP to the reflector. Now the moveout velocity recovered from the traveltimes (solid curve) practically coincides with the analytic solution for the NMO velocity (dotted curve). Therefore, the analytic and numerical results are in good agreement with each other.

Since the two models studied above exhibit such different behavior of the P-wave NMO velocity, it is important to find out what can be expected for transversely isotropic media that are likely to be encountered in the subsurface. Existing laboratory and field data indicate that in most cases $\varepsilon > \delta$ (Thomsen, 1986; Tsvankin and Thomsen, 1994). For instance, $\varepsilon > \delta$ for transversely isotropic media caused by thin bedding of isotropic layers (Berryman, 1979). This means that the cosine-of-dip corrected moveout velocity in transversely isotropic media is usually higher than the moveout velocity for a horizontal reflector [see formulas (23) and (24)]. Hence, the behavior of the corrected moveout velocity for the shale-limestone model may be typical for subsurface formations.

Rather than examine specific transversely isotropic models published in the literature, I present a systematic analysis of the P-wave DMO signatures for transversely isotropic media parametrized by ε and δ. Since the weak-anisotropy approximation suggests the difference $\varepsilon - \delta$ as the most influential parameter in the DMO correction, I generate four suites of plots for $\varepsilon - \delta = -0.1$, 0, 0.1, and 0.2 (Figures 7–10). The choice of the values of $\varepsilon - \delta$ is explained above; although $\varepsilon - \delta$ is believed to be predominantly positive, the value of -0.1 is included for completeness. Each plot contains the same three types of curves shown in Figures 5 and 6: the moveout velocity calculated from $t^2 - x^2$ curves on the spread 3000-m long (solid), the exact analytic normal-moveout velocity computed from equation (9) (dotted), and the weak-anisotropy approximation for V_{nmo} given by equation (22) (dashed). Comparison between the first two curves makes it possible to estimate the influence of nonhyperbolic moveout on the moveout velocity for the typical spread length equal to the distance from the CMP to the reflector. The difference between the second and third

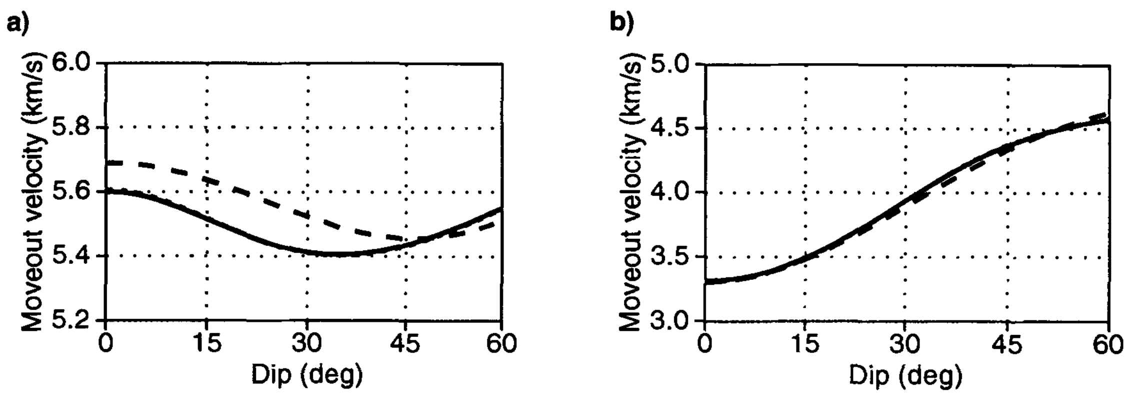

FIG. 6. Same as Figure 5 with (a) Cotton Valley shale and (b) shale-limestone, but the spread length used to calculate the moveout velocity from $t^2 - x^2$ curves (solid curve) is 1000 m instead of 3000 m. The analytic curves of the exact NMO velocity (dotted) and the weak-anisotropy approximation (dashed) have not been changed.

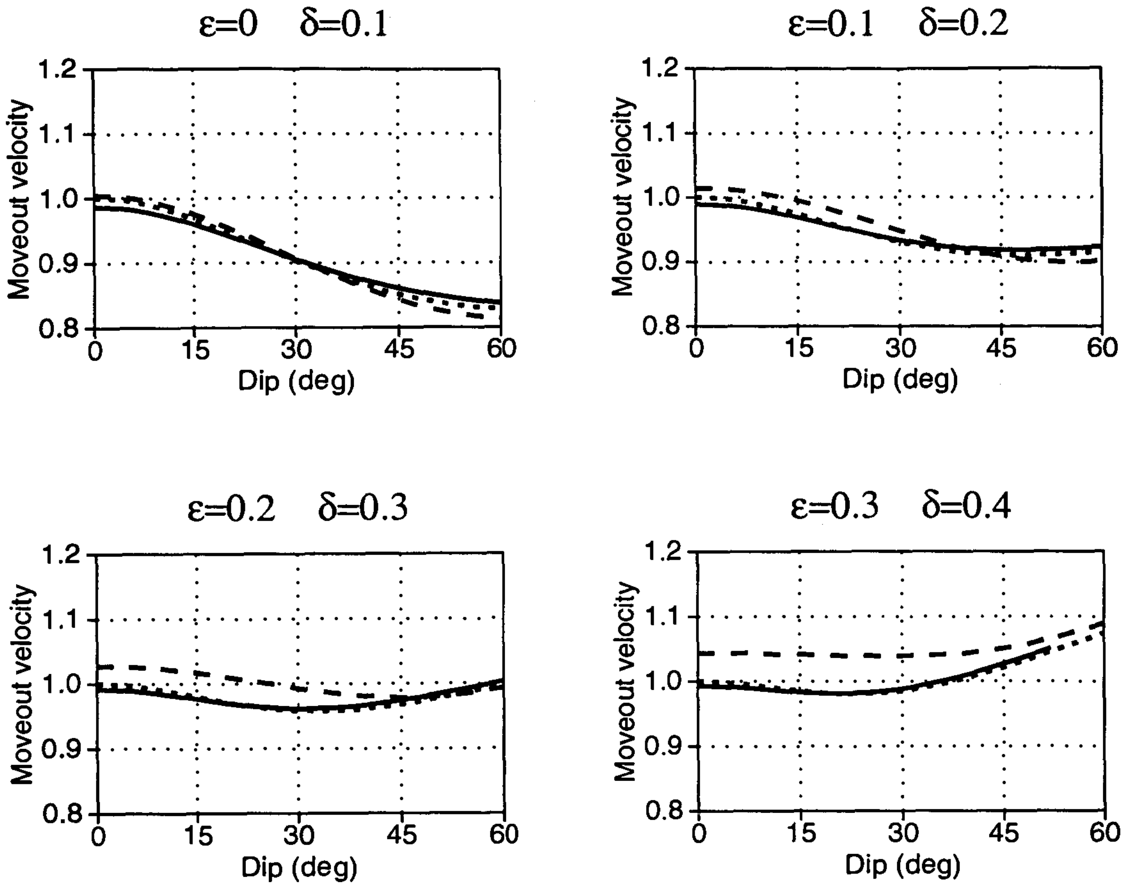

FIG. 7. Cosine-of-dip–corrected P-wave moveout velocity for models with $\varepsilon - \delta = -0.1$. The solid curve is the moveout velocity calculated from $t^2 - x^2$ curves on a spread length of 3000 m (equal to the distance between the CMP and reflector); the dotted curve is the exact NMO velocity from formula (9); and the dashed curve is the weak-anisotropy approximation from formula (22). On each plot in Figures 7–13, the vertical P-wave velocity V_{P0} is adjusted so that the exact analytic $V_{\text{nmo}}(0)$ (dotted curve) is 1 km/s. The solid curve for $\varepsilon = 0.3$, $\delta = 0.4$ stops around 52 degrees because the algorithm used to calculate traveltimes broke down at higher dips.

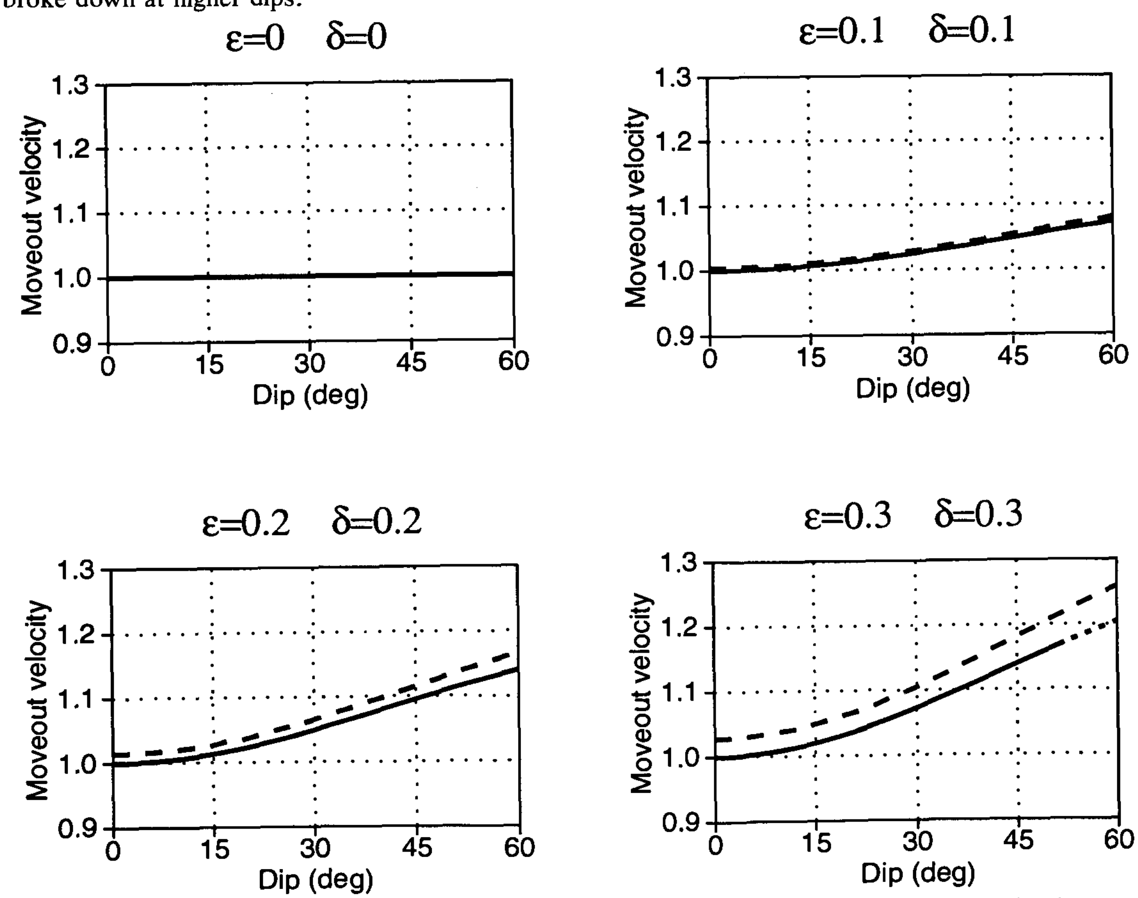

FIG. 8. Cosine-of-dip–corrected P-wave moveout velocity for models with $\varepsilon - \delta = 0$ (elliptical anisotropy).

curves shows the error of the weak-anisotropy approximation. On each plot, the vertical P-wave velocity V_{P0} is adjusted so that the exact analytic $V_{\mathrm{nmo}}(0)$ (dotted curve) is 1 km/s.

First, I examine dip-dependence of the cosine-of-dip corrected moveout velocity using the exact analytic expression (9) (dotted curve). Later on, I discuss the accuracy of the weak-anisotropy approximation and the influence of nonhyperbolic moveout.

The whole suite of plots in Figures 7–10 suggests that the P-wave DMO signature is controlled, to a significant degree (although not entirely), by the difference $\varepsilon - \delta$. In spite of certain variations from one pair of ε, δ to another, the general behavior and range of variation of the moveout velocity are similar for all curves with fixed $\varepsilon - \delta$, especially for moderate anisotropies $|\varepsilon| < 0.2$, $|\delta| < 0.2$. The dominant role of $\varepsilon - \delta$ is particularly pronounced for the most typical case $\varepsilon - \delta > 0$ (Figures 9 and 10). It is interesting that on most of the plots, the exact NMO velocity, for a fixed $\varepsilon - \delta$, shows even less dependence on a specific combination of ε and δ than does the weak-anisotropy result (for instance, see Figure 10).

When $\varepsilon - \delta = -0.1$ (Figure 7), the cosine-of-dip–corrected moveout velocity decreases with dip (for mild dips), as predicted by the weak-anisotropy approximation. This trend becomes less pronounced with increasing ε and δ because of a more significant increase in the phase velocity with angle [formula (23)]. Note that for a fixed negative $\varepsilon - \delta$, the cosine-of-dip correction becomes more accurate (i.e., the curves are closer to unity) with increasing anisotropies ε and δ. On the whole, the DMO error, determined by the amplitude of the angular variations in the cosine-of-dip–corrected moveout velocity, is relatively small (the "Cotton Valley shale" case).

For elliptically anisotropic models ($\varepsilon - \delta = 0$, Figure 8), the anisotropy-induced distortions of the cosine-of-dip dependence are entirely determined by the amplitude of the phase-velocity variations with angle. The DMO error for elliptical anisotropy is moderate: the difference between the corrected moveout velocity and the zero-dip V_{nmo} for $\phi < 60$ degrees, $|\varepsilon| < 0.2$, and $|\delta| < 0.2$ is less than 15 percent. The cosine-of-dip correction is, of course, perfect for the isotropic case, $\varepsilon = \delta = 0$.

If $\varepsilon - \delta$ is positive (the most common case, Figures 9 and 10), the anisotropy causes a pronounced increase in the cosine-of-dip–corrected moveout velocity with dip angle. Even for relatively small $\varepsilon - \delta = 0.1$, the dip-moveout error reaches 25 percent at a 45-degree dip and 30–35 percent at a dip of 60 degrees ("the shale-limestone" case). For $\varepsilon - \delta = 0.2$ (Figure 10), the corrected moveout velocity at a 60-degree dip is consistently about 60 percent higher than the zero-dip moveout velocity! A remarkable feature of models

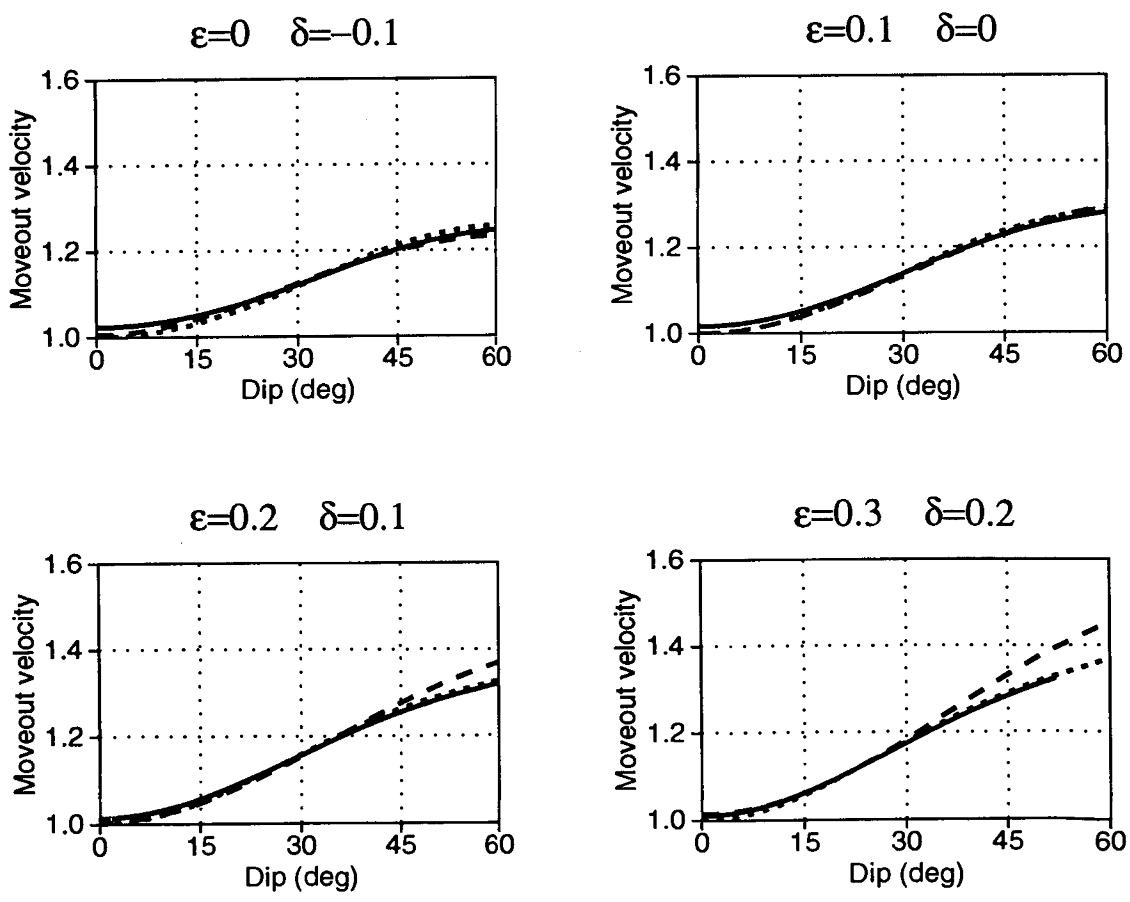

FIG. 9. Cosine-of-dip–corrected P-wave moveout velocity for models with $\varepsilon - \delta = 0.1$.

with constant positive $\varepsilon - \delta$ is the weakness of the dependence of the exact NMO velocity on ε and δ.

Thus, for typical VTI media, with positive $\varepsilon - \delta$, the isotropic cosine-of-dip correction severely understates moveout velocities at dips exceeding 20 to 30 degrees, even when the anisotropy is weak.

The range of dips on the plots above was limited to 60 degrees. For typical models with $\varepsilon - \delta > 0$, curves of the cosine-of-dip–corrected moveout velocity flatten out at dip angles exceeding 60 degrees (Figure 11). Therefore, the error of the cosine-of-dip dependence remains practically constant at steep dips in the 60–90 degree range.

The weak-anisotropy approximation for the normal-moveout velocity given by equation (22) remains sufficiently accurate in the most important range of small and moderate values of ε and δ. The error of the weak-anisotropy result, as compared with the exact NMO velocity from equation (9), does not exceed 5 percent for $|\varepsilon| \leq 0.2$, $|\delta| \leq 0.2$ (the only exception is the model with $\varepsilon = 0$, $\delta = -0.2$).

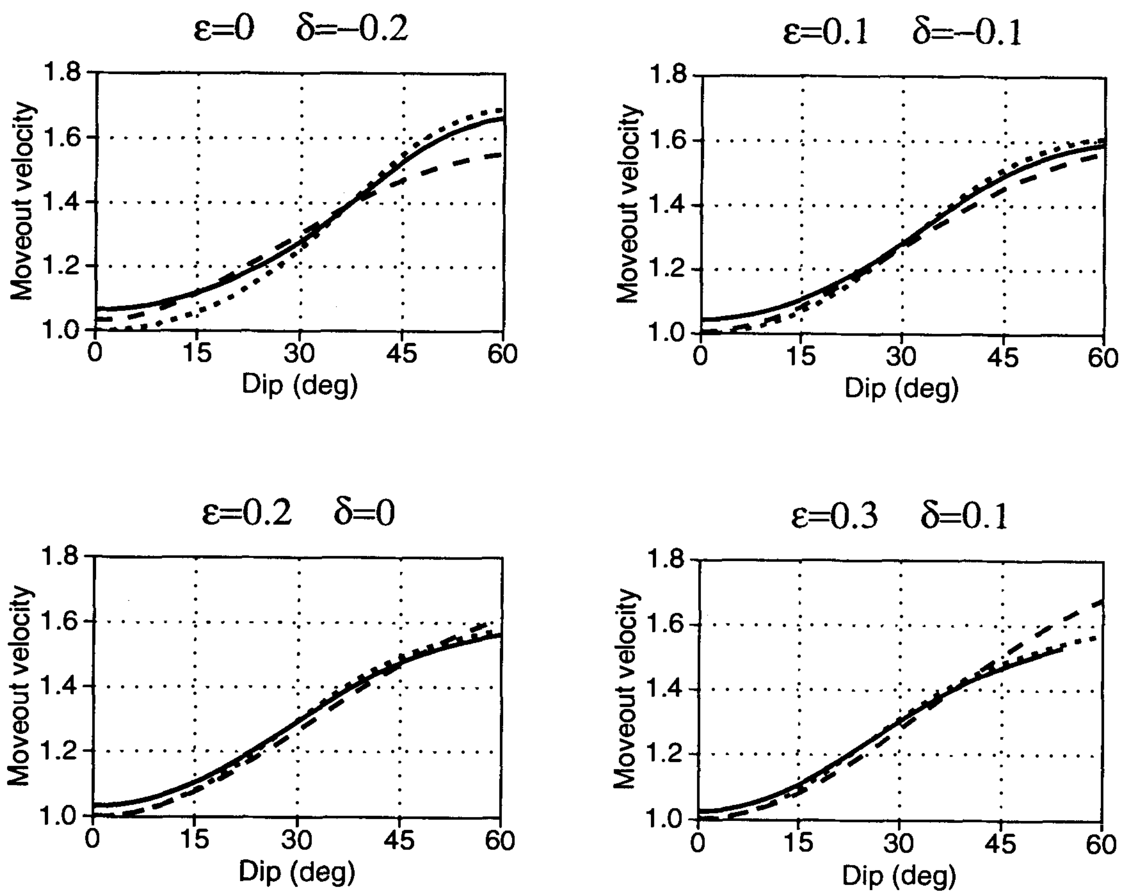

FIG. 10. Cosine-of-dip–corrected P-wave moveout velocity for models with $\varepsilon - \delta = 0.2$.

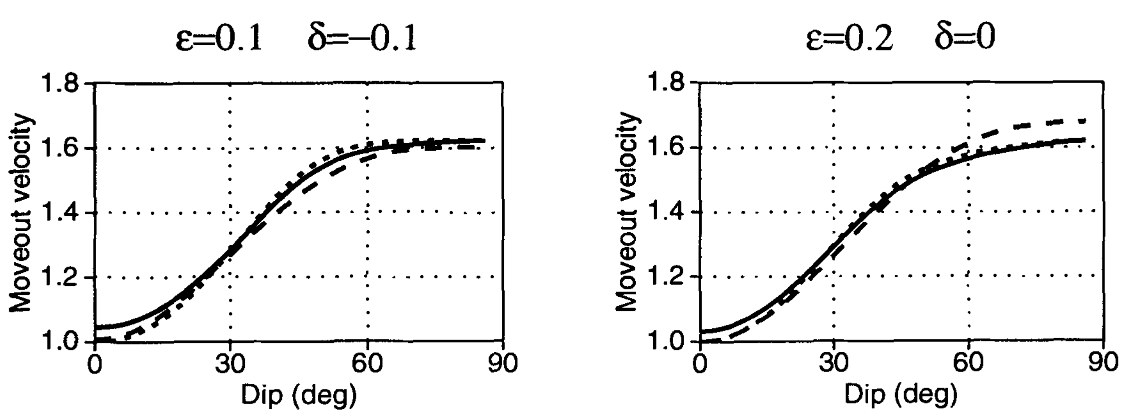

FIG. 11. Cosine-of-dip–corrected P-wave moveout velocity for steep reflectors; $\varepsilon - \delta = 0.2$.

The above suite of plots also presents a comprehensive picture of the moveout-velocity distortions at various dips caused by nonhyperbolic moveout. The influence of nonhyperbolic moveout manifests itself through the difference between the moveout velocity, calculated from $t^2 - x^2$ curves (solid curves), and the exact NMO velocity (dotted curves). It is well known that deviations from hyperbolic moveout rapidly increase with spread length; this trend may be enhanced by anisotropy (Tsvankin and Thomsen, 1994). For a maximum offset-to-depth ratio of 1, used in my calculations, the contribution of nonhyperbolic moveout to the moveout velocity is not significant, but the difference between the NMO and finite-spread velocities is clearly visible on some of the plots.

For small dips, the distortions of the moveout velocity caused by deviations from hyperbolic moveout are in good agreement with the analytic results in Tsvankin and Thomsen (1994) who gave a description of nonhyperbolic moveout for horizontal reflectors using the quartic Taylor series term for $t^2 - x^2$ curves. For the P-wave, the influence of nonhyperbolic moveout is largely proportional to the absolute value of $\varepsilon - \delta$; if $\varepsilon - \delta$ is fixed, nonhyperbolic moveout is more pronounced for smaller δ. The analytic analysis also shows that the P-wave moveout velocity measured on finite spreads is larger than the NMO velocity if $\varepsilon - \delta > 0$, and smaller than V_{nmo} if $\varepsilon - \delta < 0$. The validity of these conclusions is clearly seen in Figures 7–10. For elliptical anisotropy ($\varepsilon = \delta$) the moveout is purely hyperbolic, and the dotted and solid curves fully coincide with each other.

The observed differences between the NMO velocity and the finite-spread moveout velocity seem to contradict the results in Levin (1990) and Larner (1993), who have not noticed visible deviations of their moveout curves from hyperbolas for the same spread length. However, this is an apparent discrepancy. Tsvankin and Thomsen (1994) show that for spread lengths close to the depth of the reflector, the best-fit hyperbola is close to the actual moveout curve although the moveout velocity of this hyperbola may be different by several first percent from the NMO velocity.

It is interesting that the difference between the moveout velocity on a finite spread and the NMO velocity changes sign with increasing dip (i.e., the solid and dotted lines cross); moreover, the influence of nonhyperbolic moveout for steep reflectors is typically smaller than for zero dip (e.g., Figure 11). I conclude that if $|\varepsilon - \delta| < 0.15$–$0.2$, nonhyperbolic moveout does not seriously distort the P-wave moveout velocity on spreads common for CMP acquisition design, even if dips are large.

Apparent versus true dip

In the discussion above, we have not made a distinction between the true dip angle and an apparent dip used in constant-velocity DMO. Since the true dip is usually unknown, NMO velocity is conventionally expressed through ray parameter p as

$$V_{\text{nmo}}(p) = \frac{V_{\text{nmo}}(0)}{\sqrt{1 - p^2 V_{\text{nmo}}^2(0)}}, \tag{26}$$

where p is determined from the zero-offset section $t_0(y)$:

$$p = \frac{dt_0}{dy} = \frac{\sin\phi}{V(\phi)},$$

where $V(\phi)$ is the phase velocity at the dip angle. This expression for p is valid for both isotropic and anisotropic media.

Equation (26) implies that the true dip angle ϕ is replaced in the DMO correction with the apparent dip $\hat{\phi}$ (Larner, 1993)

$$\sin\hat{\phi} = pV_{\text{nmo}}(0) = \sin\phi\,\frac{V_{\text{nmo}}(0)}{V(\phi)}. \tag{27}$$

In a homogeneous isotropic medium $V_{\text{nmo}}(0) = V_0 = V(\phi)$, and the apparent and true dip angles coincide with each other. If the medium is vertically transversely isotropic, the zero-dip normal-moveout velocity given by equation (17) (for P-waves) is generally different from the phase velocity at the dip angle $V(\phi)$. This means that substituting the apparent dip for the true dip in the presence of anisotropy introduces an additional error into a constant-velocity DMO process. In principle, this new error may either reinforce or reduce the error in moveout velocity discussed above.

As shown in Figures 12 and 13, the DMO correction using the apparent dip leads to higher DMO errors for both $\varepsilon - \delta > 0$ and $\varepsilon - \delta < 0$, especially at steep dips ($\phi > 45$ degrees). Note that after the correction for the apparent dip, moveout velocities for models with the same $\varepsilon - \delta$ remain close if $\varepsilon - \delta > 0$ and become even closer if $\varepsilon - \delta < 0$.

The only class of models for which the introduction of the apparent dip has a benign influence on the overall DMO performance is elliptical anisotropy ($\varepsilon - \delta = 0$). It is interesting that for elliptical models the correction of moveout velocity with $\cos\hat{\phi}$ instead of $\cos\phi$ eliminates the DMO error completely (Figure 12); this result is easy to confirm analytically using equation (27) and velocity equations for elliptical anisotropy. Thus, the isotropic constant-velocity DMO correction is exact for elliptically anisotropic models, of which isotropic models are a special case.

TRANSVERSELY ISOTROPIC MEDIA WITH VERTICAL VELOCITY GRADIENT

The analysis in the previous sections was carried out for homogeneous transversely isotropic models. Larner (1993) has studied the P-wave dip-moveout error for factorized VTI media with a constant gradient in vertical velocity. In terms of the notation used here, the velocity V_{P0} in factorized transversely isotropic media varies with position, while the V_{P0}/V_{S0} ratio and the anisotropic coefficients ε and δ remain constant. The four models used in Larner's work have the same anisotropic parameters and root-mean-square (rms) vertical velocity down to the reflector as the models in Levin's (1990) study. One of the interesting results reported by Larner is that for the shale-limestone model with a typical value of the velocity gradient, the constant-velocity (cosine-of-dip) DMO correction gives a higher accuracy than does $V(z)$ DMO (both DMO corrections ignore anisotropy). Comparison of the moveout velocities for homogeneous and inhomogeneous shale-limestone suggests that inhomogeneity can compensate (to a certain degree) for the distortions of moveout velocity caused by the anisotropy.

The results obtained in the previous section indicate that the behavior of NMO velocity for the homogeneous shale-limestone may be considered typical for a wide range of VTI models. To verify whether the "compensation effect," found by Larner, is typical for inhomogeneous (factorized) VTI media, I carry out the same calculations as in the previous section, but for factorized transversely isotropic media with a vertical velocity gradient of 0.6 s^{-1} (Figure 14). The moveout velocity is calculated from $t^2 - x^2$ curves using Larner's (1993) ray-tracing algorithm.

Comparison of Figure 14 with Figures 9 and 10 shows that for typical positive values of $\varepsilon - \delta$, angular variations of the cosine-of-dip-corrected moveout velocity are substantially suppressed by the velocity gradient. It is noteworthy that Larner and Cohen (1993) have found a similar "compensation effect" in their study of migration error in factorized transversely isotropic media. When velocity increases with depth, small-offset reflections from dipping interfaces travel more closely to vertical than in a homogeneous medium. This makes the "effective dip" of the reflector smaller and reduces the increase in the moveout velocity with dip angle, both in isotropic and anisotropic media. For $\varepsilon - \delta = 0.1$, the influence of vertical velocity variations even leads to "over-correction" in constant-velocity DMO, making the cosine-of-dip-corrected moveout velocity decrease with dip angle.

Figure 14 is reproduced in Figure 15, but with the DMO correction that honors inhomogeneity but ignores anisotropy [$V(z)$ DMO, Larner (1993)]. Although the DMO error caused by the anisotropy is somewhat smaller than in homogeneous media with the same ε and δ (Figures 9 and 10), it is much larger than the error of the simplest cosine-of-dip correction (Figure 14). Therefore, consistent with Larner's results for the shale-limestone model, for typical factorized transversely isotropic models the DMO correction that ignores both anisotropy and inhomogeneity is often more accurate than the correction that honors inhomogeneity but ignores anisotropy. Another important conclusion from Figures 14 and 15 is that in factorized vertically inhomogeneous VTI media, the P-wave moveout velocity is still controlled primarily by the difference between ε and δ, rather than by the individual values of these parameters. However, in $V(z)$ media, dip dependence of the moveout velocity is also a function of the velocity gradient, the rms vertical velocity, and the depth of the reflector. As illustrated by Figure 16, for more shallow reflectors the influence of the velocity gradient is less pronounced, and the corrected

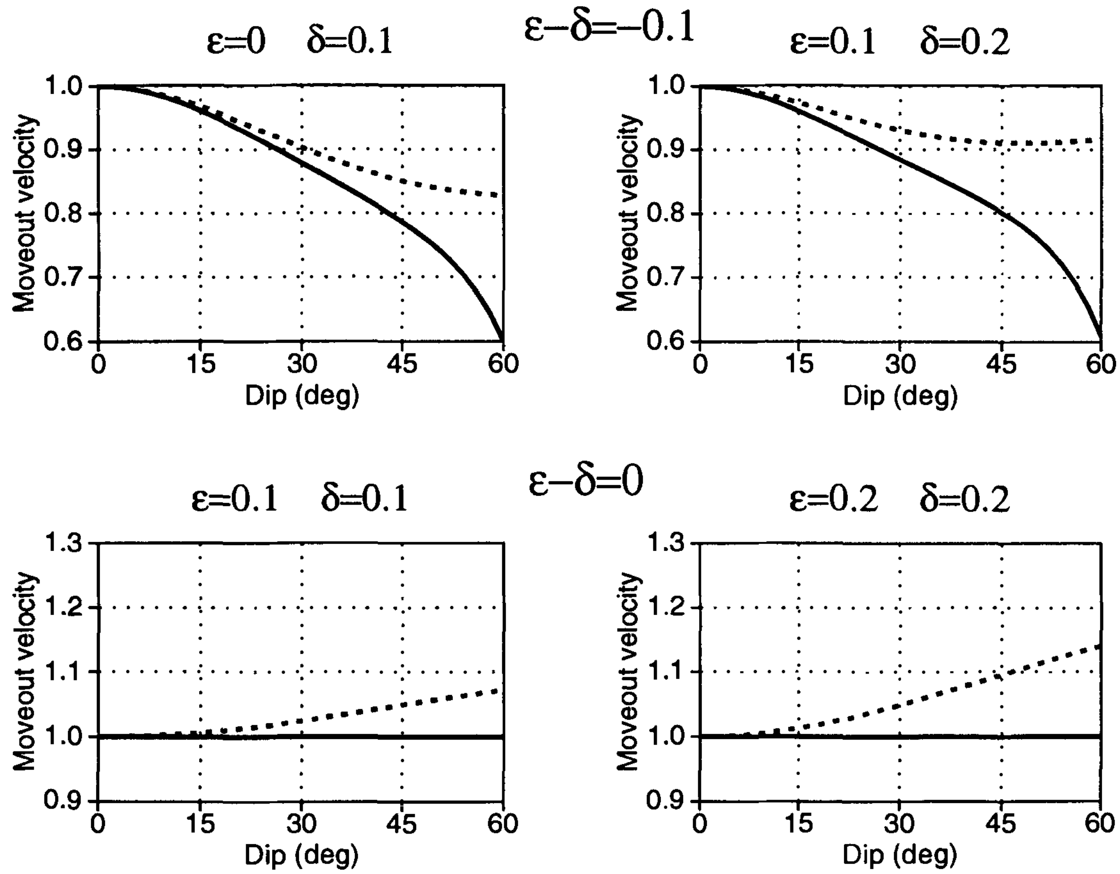

FIG. 12. Comparison of DMO corrections using the true and apparent dip angles for models with $\varepsilon - \delta \leq 0$. P-wave normal-moveout velocity is calculated from formula (9) and corrected with the cosine of the true dip angle ϕ (dotted curves, same as in Figures 7–10) and the apparent angle $\hat{\phi}$ from equation (27) (solid curves).

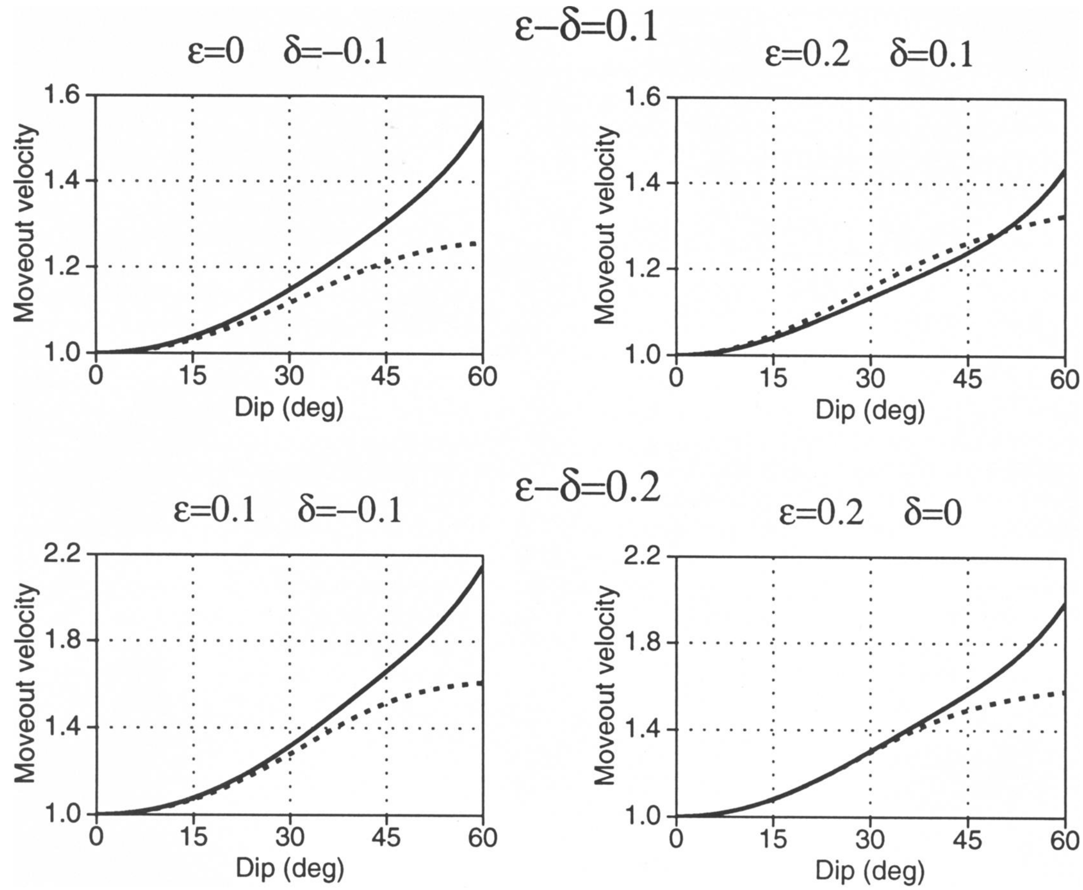

FIG. 13. Comparison of DMO corrections using the true (dotted curve) and apparent (solid curve) dip angles for $\varepsilon - \delta > 0$.

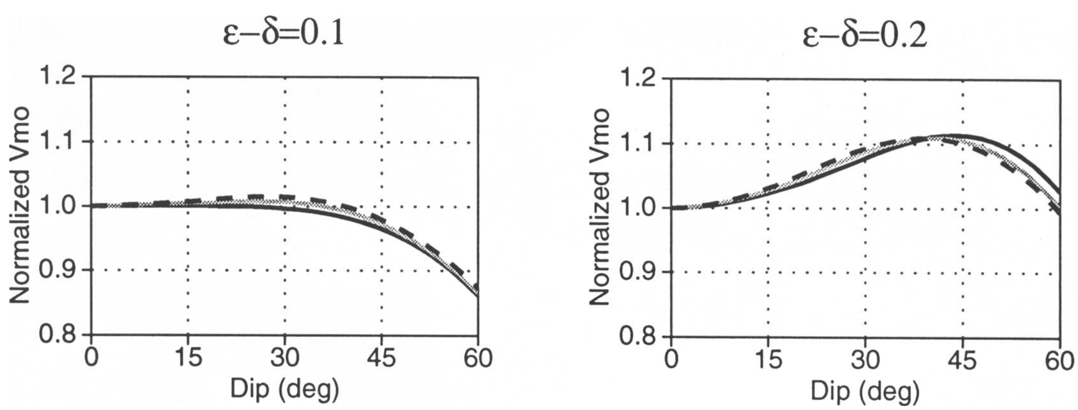

FIG. 14. *P*-wave moveout velocity corrected for the cosine of the true dip angle for VTI models with a velocity gradient of 0.6 s^{-1}. The curves are normalized by the moveout velocity for a horizontal reflector. Each curve corresponds to a different pair of ε, δ. On the left plot, $\varepsilon = 0$, $\delta = -0.1$ (black curve); $\varepsilon = 0.1$, $\delta = 0$ (gray curve); $\varepsilon = 0.2$, $\delta = 0.1$ (dashed curve). On the right plot, $\varepsilon = 0.1$, $\delta = -0.1$ (black curve); $\varepsilon = 0.2$, $\delta = 0$ (gray curve); $\varepsilon = 0.3$, $\delta = 0.1$ (dashed curve). The distance from the CMP to the reflector and the spread length are 3000 m; the rms vertical velocity down to 3000 m is 3500 m/s.

moveout velocity is closer to the result for a homogeneous medium. It is interesting that for the rather typical model parameters used in the left portion of Figure 16, the anisotropy and inhomogeneity cancel each other's influence, and the cosine-of-dip formula yields almost an ideal correction.

So far in this section the DMO error has been estimated using the true dip angle ϕ. The simplistic constant-velocity DMO approach, described in the previous section, would result in the apparent dip $\hat{\phi}$ given by equation (27):

$$\sin \hat{\phi} = \sin \phi \, \frac{V_{\text{nmo}}(z_0, 0)}{V(z_1, \phi)}, \tag{28}$$

where the velocities V_{nmo} and V in FTI media depend on the depths of the zero-offset reflection points z_0 (for the horizontal reflector) and z_1 (for the dipping reflector).

For models with $\varepsilon - \delta > 0$, the apparent dip angle turns out to be smaller than the true one and, consequently, the cosine-of-dip–corrected moveout velocity becomes larger (compare Figure 17 with Figure 14). If $\varepsilon - \delta = 0.2$, the introduction of the apparent dip may lead to much higher errors in constant-velocity DMO and a noticeable separation of curves corresponding to different pairs of ε, δ. For $\varepsilon - \delta = 0.1$, the difference between the apparent and true dip angles is somewhat smaller.

In analyzing these results, one should keep in mind that the computation of the apparent dip in FTI media using equation (28) is strongly dependent on the relative spatial positions of the horizontal and dipping reflectors. The results in Figure 17 are obtained for the reflectors located at the same distance from the CMP point. If, instead, we compare the moveout velocities of reflectors at the same zero-offset time, the apparent dip usually becomes much closer to the true one.

DISCUSSION

In the presence of anisotropy, the dip dependence of moveout velocity deviates from the isotropic cosine-of-dip function, thus leading to errors in conventional isotropic DMO correction. Here, I have given an analytic description of NMO velocities that provides a clear explanation for existing numerical results, such as Levin's (1990) conclusion that the cosine-of-dip dependence of moveout velocity remains valid for transverse isotropy if the symmetry axis is perpendicular to the reflector.

Transversely isotropic models with a vertical symmetry axis (VTI media) were considered in most detail. A simple weak-anisotropy approximation, derived from the exact NMO expression, relates the distortions of NMO velocity to the anisotropic parameters. The weak-anisotropy expression for the P-wave normal-moveout velocity is sufficiently accurate for common small and moderate values of ε and δ. The error of the weak-anisotropy result usually does not exceed 5 percent for $|\varepsilon| \leq 0.2$, $|\delta| \leq 0.2$.

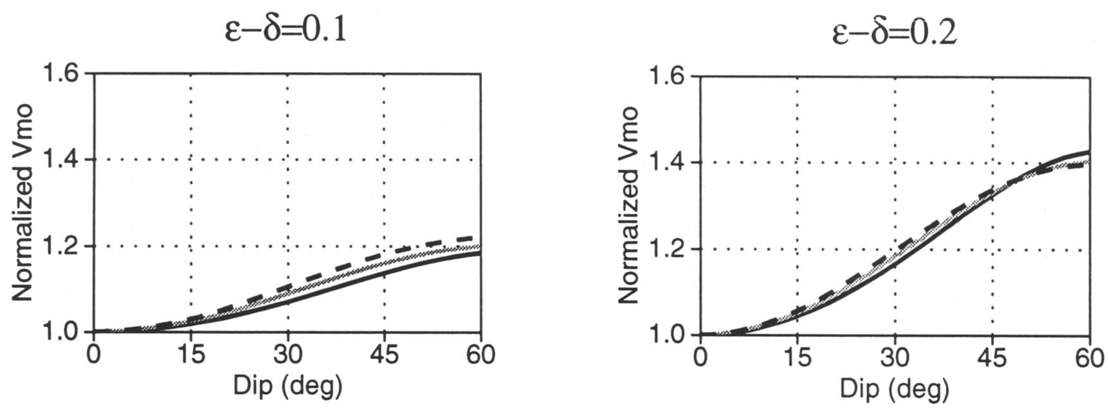

FIG. 15. P-wave moveout velocity after $V(z)$ DMO correction. All parameters are the same as in Figure 14.

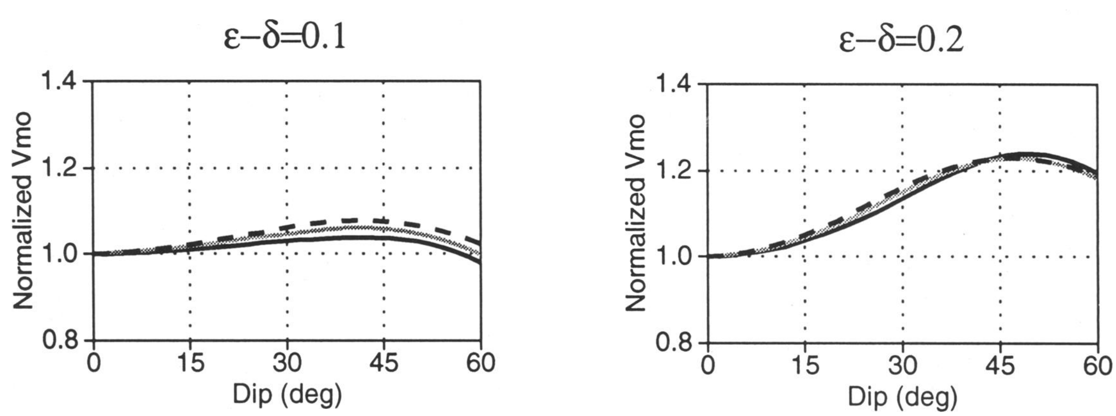

FIG. 16. Cosine-of-dip–corrected P-wave moveout velocity for the same elastic parameters as in Figure 14, but for a more shallow reflector: the distance from the CMP to the reflector and the spread length are 1500 m.

Dip dependence of the P-wave moveout velocity for VTI media is a function of only two parameters–ε and δ, with the influence of the S-wave vertical velocity V_{S0} being practically negligible. More than that, the P-wave DMO signature is controlled, to a significant degree, by the difference $\varepsilon - \delta$. The systematic study of VTI media parameterized by ε and δ shows that for $\varepsilon - \delta > 0$ (the most common case), the cosine-of-dip–corrected moveout velocity remains significantly larger than the moveout velocity for a horizontal reflector. Even for relatively small $\varepsilon - \delta = 0.1$ and $\varepsilon \le 0.2$, the error of the cosine-of-dip formula reaches 25 percent at a 45-degree dip and exceeds 30 percent at a dip of 60 degrees. For $\varepsilon - \delta = 0.2$ (also a feasible value), the cosine-of-dip–corrected moveout velocity at 60-degree dip is almost 60 percent higher than the zero-dip moveout velocity. The DMO errors become even higher if the true dip angle is replaced with the apparent dip calculated from the conventional formula used in constant-velocity DMO.

The analytic study of NMO velocities was supplemented by calculations of the P-wave moveout velocity from reflection $t^2 - x^2$ curves on relatively short-spread CMP gathers (i.e., spread length ≈ distance between CMP and reflector), typical for CMP acquisition design. Comparison between the analytic NMO velocity and the moveout velocity calculated on finite spreads makes it possible to analyze the magnitude of nonhyperbolic moveout (induced by the anisotropy) as a function of reflector dip. The difference between the two velocities changes sign with increasing dip, but is usually smaller for large dips than for horizontal reflectors. If $|\varepsilon - \delta| < 0.15$–$0.2$, nonhyperbolic moveout does not seriously distort the P-wave moveout velocity on conventional length spreads, even for steep reflectors.

Significant errors of conventional cosine-of-dip DMO correction for typical transversely isotropic models mean that it is imperative to develop dip-moveout algorithms for anisotropic media. Uren et al. (1990a) have generalized Gardner DMO for elliptically anisotropic models; however, as shown in the present paper, the elliptical P-wave DMO correction becomes inaccurate even for "almost" elliptically anisotropic models. The formula for NMO velocity, derived here, can provide a basis for building DMO algorithms for general transversely isotropic and even orthorhombic media.

One of the major problems in developing dip-moveout processing (as well as migration, amplitude variation with offset algorithms, etc.) in anisotropic media is recovery of the input anisotropic parameters with sufficient accuracy. For VTI media, the parameter δ can be determined using the P-wave NMO velocity from a horizontal reflector and the true vertical velocity (such as from check shots or VSP data). However, the parameter ε cannot be recovered from short-spread P-wave data alone. If the vertical P- and/or S-velocities (or reflector depth) are known, both ε and δ can be determined from the P- and SV-wave NMO velocities. Tsvankin and Thomsen (1995) show that it is possible to find all four anisotropic parameters governing P-SV propagation (V_{P0}, V_{S0}, ε, δ) from the combination of long-spread P- and SV-traveltimes; however, this algorithm is not easy to implement in practice. Since ε is directly related to the horizontal velocity, it can also be determined from head-wave velocities or results of crosshole tomography.

Another way to overcome the ambiguity in the recovery of the anisotropic parameters is to include moveout from dipping reflectors in the inversion procedure. Application of the analytic NMO formula developed here to inversion in anisotropic media will be discussed in a sequel paper.

CONCLUSIONS

I have introduced an analytic expression for normal-moveout velocity from dipping reflectors valid in symmetry planes of homogeneous arbitrary-anisotropic media. The new formula describes NMO velocities of P- and S-waves in many anisotropic models of practical importance, such as transverse isotropy with an in-plane symmetry axis, and symmetry planes in orthorhombic media.

The dip dependence of P-wave NMO velocity in VTI media is determined more by the difference between the parameters ε and δ, than by the individual values of the anisotropic coefficients. For the most common case, $\varepsilon - \delta > 0$, the NMO velocity increases with dip much faster than in isotropic media, even for models with moderate $\varepsilon - \delta = 0.1$ to 0.2. This implies that conventional constant-velocity DMO algorithms, based on the isotropic cosine-of-dip de-

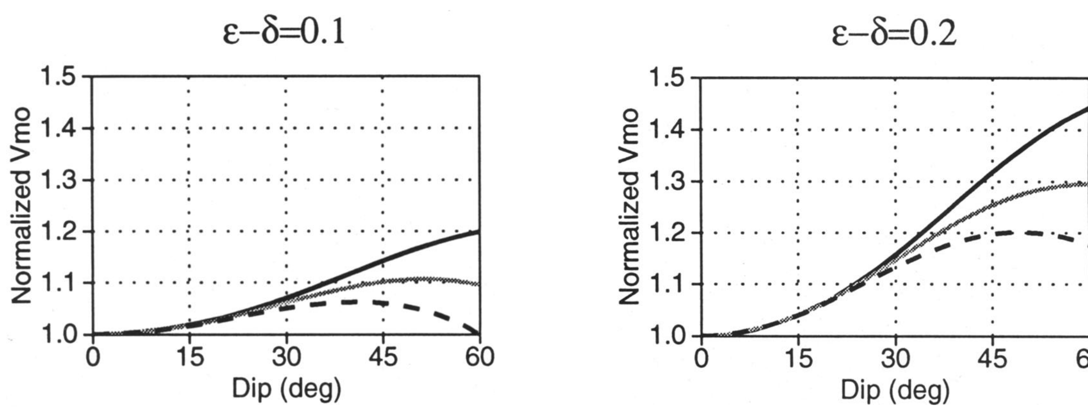

FIG. 17. P-wave moveout velocity corrected with the cosine of the apparent dip angle $\hat{\phi}$. All parameters are the same as in Figure 14.

pendence, are subject to significant errors in transversely isotropic media.

Deviations of P-wave NMO velocity from the cosine-of-dip dependence are much less pronounced for factorized VTI media with positive $\varepsilon - \delta$ and an increase in vertical velocity with depth, than for homogeneous media. Therefore, if a medium is not only anisotropic, but also has a vertical-velocity gradient, isotropic constant-velocity DMO can perform better than can be expected from the results for homogeneous anisotropic media.

In principle, the expression for normal-moveout velocity derived here can be used for only the short-spread (hyperbolic) portion of the moveout curve. However, analysis of moveout velocity on conventional spreads close to the distance between the CMP and the reflector shows that the magnitude of anisotropy-induced nonhyperbolic moveout for P-waves is relatively small and tends to decrease at steep dips.

The formula for NMO velocity derived in the paper provides a basis for building dip-moveout algorithms in anisotropic media. It can also be used to overcome the ambiguity in the inversion of reflection moveouts for anisotropic parameters by including dip dependence of moveout velocities in the inversion procedure.

ACKNOWLEDGMENTS

I am grateful to Ken Larner for many helpful discussions, for use of his ray-tracing code, and for his thorough review of the paper. I would like to thank the reviewers for useful comments and John Anderson (Mobil) for his insight into the character of DMO performance. The support for this work was provided by the members of the Consortium Project on Seismic Inverse Methods for Complex Structures at the Center for Wave Phenomena (CWP), Colorado School of Mines, and by the United States Department of Energy, Grant Number DE-FG02-89ER14079 (this support does not constitute an endorsement by DOE of the views expressed in this paper).

REFERENCES

Banik, N. C., 1984, Velocity anisotropy of shales and depth estimation in the North Sea Basin: Geophysics, **49**, 1411–1419.
Berryman, J. G., 1979, Long-wave elastic anisotropy in transversely isotropic media: Geophysics, **44**, 896–917.
Byun, B., 1982, Seismic parameters for media with elliptical velocity dependencies: Geophysics, **47**, 1621–1626.
——— 1984, Seismic parameters for transversely isotropic media: Geophysics, **49**, 1908–1914.
Hake, H., Helbig, K., and Mesdag, C. S., 1984, Three-term Taylor series for $t^2 - x^2$ curves over layered transversely isotropic ground: Geophys. Prosp., **32**, 828–850.
Hale, D., and Artley, C., 1993, Squeezing dip moveout for depth-variable velocity: Geophysics, **58**, 257–264.
Hale, D., Hill, N. R., and Stefani, J., 1992, Imaging salt with turning seismic waves: Geophysics, **57**, 1453–1462.
Hubral, P., and Krey, T., 1980, Interval velocities from seismic reflection time measurements: Soc. Expl. Geophys.
Larner, K., 1993, Dip-moveout error in transversely isotropic media with linear velocity variation in depth: Geophysics, **58**, 1442–1453.
Larner, K., and Cohen, J., 1993, Migration error in factorized transversely isotropic media with linear velocity variation with depth: Geophysics, **58**, 1454–1467.
Leary, P. C., Crampin, S., and McEvilly, T. V., 1990, Seismic fracture anisotropy in the Earth's crust: An overview: J. Geophys. Res., **95**, B7, 11 105–11 114.
Levin, F. K., 1971, Apparent velocity from dipping interface reflections: Geophysics, **36**, 510–516.
——— 1990, Reflection from a dipping plane—Transversely isotropic solid: Geophysics, **55**, 851–855.
Sams, M. S., Worthington, M. H., and Khanshir, M. S., 1993, A comparison of laboratory and field measurements of P-wave anisotropy: Geophys. Prosp., **41**, 189–206.
Thomsen, L., 1986, Weak elastic anisotropy: Geophysics, **51**, 1954–1966.
Tsvankin, I., and Thomsen, L., 1994, Nonhyperbolic reflection moveout in anisotropic media: Geophysics, **59**, 1244–1258.
——— 1995, Inversion of reflection traveltimes for transverse isotropy: Geophysics, (Scheduled for publication in September).
Uren, N. F., Gardner, G. N. F., and McDonald, J. A., 1990a, Dip moveout in anisotropic media: Geophysics, **55**, 863–867.
——— 1990b, Normal moveout in anisotropic media: Geophysics, **55**, 1634–1636.
White, J. E., 1983, Underground sound: Application of sound waves: Elsevier Science Publ.